A New Noninvasive System for Clinical Pulse Wave Velocity Assessment: The Athos Device

A new noninvasive system for clinical Pulse Wave Velocity assessment: the Athos device

Irene Buraioli, Davide Lena, Giulia Mingrone, Alberto Milan* and Danilo Demarchi*, *Senior Member, IEEE*

***Abstract*— This paper presents a low cost, noninvasive, clinical-grade Pulse Wave Velocity evaluation device. The proposed system relies on a simultaneous acquisition of femoral and carotid pulse waves to improve estimation accuracy and correctness. The sensors used are two high precision MEMS force sensors, encapsulated in two ergonomic probes, and connected to the main unit. Data are then wirelessly transmitted to a standard laptop, where a dedicated graphical user interface (GUI) runs for analysis and recording. Besides the interface, the Athos system provides a Matlab algorithm to process the signals quickly and achieve a reliable PWV assessment. To better compare the results at the end of each analysis, a detailed report is generated, including all the relevant examination information (subject data, mean PTT, and obtained PWV).**

A pre-clinical study was conducted to validate the system by realizing several Pulse Wave Velocity measurements on ten heterogeneous healthy subjects of different ages. The collected results were then compared with those measured by a well-established and largely more expensive clinical device (SphygmoCor).

***Index Terms*— Arterial stiffness, tonometry, arterial pulse, Pulse Wave Velocity, Pulse Transit Time, intersecting tangent algorithm**

I. Introduction

CARDIOVASCULAR Diseases (CVDs) are a group of illnesses that involve both the heart and the circulatory system. A strictly correlated parameter with the state of the cardiovascular system is the large arterial stiffness [1]. This has become one of the most important classifiers for cardiovascular pathologies. Particularly, the arterial stiffness is bonded with the elastic properties of the vessels, and it plays an essential role with the systolic blood pressure. In turn, a high arterial stiffness could lead to cardiac hypertrophy and arterial lesions [2]–[4]. Nowadays, several methods have been addressed to quantify arterial stiffness using a noninvasive approach [5]–[9].

One way to assess the elastic property of the arterial tree is the Pulse Wave Velocity (PWV), that corresponds to the velocity at which blood pulse propagates through the cardiovascular system. The higher the PWV, the stiffer the blood vessel walls. Moreover, for the first time in 2018, in the European Society of Cardiology and Hypertension guidelines appeared the PWV as a significant predictor of cardiovascular risk stratification and useful for identifying asymptomatic organ damage (OD) [10].

Usually, this velocity could be evaluated considering two sites among the cardiovascular system but, according to the "Expert consensus document on arterial stiffness", the carotid-femoral PWV (cf-PWV) is the noninvasive gold standard for this type of measurement [11]. Indeed, with the cf-PWV, there is the possibility to evaluate the aorta's elasticity, which is the most exposed artery to risk factors and aging.

In the clinical noninvasive cf-Pulse Wave Analysis, the carotid pulse, close to the neck, is associated with the heart blood ejection action on each cardiac cycle. While the femoral pulse, located midway between the anterior superior iliac spine and the symphysis pubis, is chosen as the peripheral site. A specific distance d separates these sites, which corresponds to the path length through the arterial tree. It is approximately estimated with the direct measure of the distance between proximal and distal points. The time needed by the pulse to propagate between these two sites is called the delay or Pulse Transit Time (PTT). The PWV parameter is computed as the linear ratio between d and the PTT, as follow:

$$PWV = \frac{distance}{PTT} \quad (1)$$

Nowadays, several devices exist to assess this cardiovascular parameter [12], very few of them are portable as in [13]. They differ for the methodology and the procedure used to evaluate the PWV. Regarding the methodology, typically the most used and reliable approach is the applanation tonometry, followed by cuff-based oscillometry [14] and optical sensors. Instead, the procedure comprises the actions needed by the instrument's user to address the PTT evaluation, and it depends on the presence of the electrocardiogram (ECG) signal in the system. Basically, two types of PWV extraction could be distinguished: the *one-*

Manuscript received November **, 2020; revised November **, 2020; accepted **** **, 2020. Date of publication **** **, 2020; date of current version **** **, 2020. This work was supported by PolitoBIOMed Lab-Biomedical Engineering Lab.

I. Buraioli and D. Demarchi are with the Department of Electronics and Telecommunications, Politecnico di Torino, 10129 Torino, Italy, (e-mail: irene.buraioli@polito.it; danilo.demarchi@polito.it).

D. Lena is with STMicroelectronics, 20010 Cornaredo, Italy (e-mail: davide.lena@st.com).

G. Mingrone and A. Milan are with Department of Medical Sciences, Internal Medicine and Hypertension Division, University of Torino – AOU Città della Salute e della Scienza di Torino, 10126 Torino, Italy, (e-mail: giulia.mingrone@edu.unito.it; alberto.milan@gmail.com).

* These authors are joint last authors: Alberto Milan and Danilo Demarchi

step and the *two-steps* methods. The *two-steps* method involves both the ECG and arterial pulse signals. In the first phase, the time employed by the blood pulse to propagate from the heart (ECG reference) to the carotid (pulse detection) is taken as carotid Pulse Transit Time (cPTT). Then, in a second moment, the propagation time from the heart (ECG reference) to the femoral site (pulse detection) is recorded as femoral Pulse Transit Time (fPTT). Finally, the PTT considered for the PWV evaluation is the difference between the two acquired intervals (cfPTT= fPTT - cPTT). On the other hand, the *one-step* method consists of a single simultaneous acquisition of the pulse wave on carotid and femoral sites, without the ECG's need, so directly evaluating the differential PTT.

Concerning the clinical extraction of the pulse wave velocity, many devices are available in the medical segment. The reference instrument for the noninvasive PWV measurement is the SphygmoCor (AtCor Medical, Sydney, Australia). It is based on piezoelectric force sensors, and it analyses the pulse wave of carotid and femoral arteries following the *two-steps* approach [15]. Another commercial device is the PulsePen (DiaTecne, Milan, Italy), composed of one tonometer and an integrated ECG unit. The carotid and femoral pulse waves are acquired in *two-steps* by applanation tonometry, both synchronized with the ECG R peak [16]. The third device is the Complior (Alam Medical, Saint Quentin Fallavier, France), which uses two dedicated piezoelectric pressure mechanotransducers directly applied to the skin in a simultaneous acquisition of pressure pulses [17]. Table 1 summarizes the three more used PWV systems' main characteristics compared with the presented Athos. As it could be seen, the proposed device could play a significant role since it is more than favorable in all the underlined aspects, introducing a custom project that implements newer and less expensive technology.

The Athos (Arterial sTiffness faitHful tOol aSsessment) system for noninvasive Pulse Wave Velocity evaluation will be presented in this paper. As said before, despite the actual devices that address the same cardiovascular parameter, it has several advantages. (a) It performs the one-step PWV assessment, but it also allows the two-steps method implementation through the addition of a clinical-grade compatible electrocardiograph. (b) It is equipped with two Micro Electro-Mechanical Systems (MEMS) pressure sensors encapsulated in two pen-shaped supports to simplify the clinical operator usage and increase instrument portability. (c) The Athos system has a graphical software interface that conducts the users through a reliable PWV extraction. (d) Thanks to the cooperation with the medical staff of the "Città della Salute e della Scienza" Hospital in Turin (Italy), the system has been optimized to give high performances and to be easily usable. (e) The main obstacle to the spread of the arterial stiffness evaluation through cf-PWV in the clinical practice is due to the too high cost of the equipment with a not easy usability. For this reason, the main aim of the Athos system is to introduce an affordable system that reliably assesses PWV, and it is built with components chosen off the shelf. Thus, the main advantages of Athos are to be cost-effective and to have an optimized smart system for portability and easy management.

TABLE I
SYSTEMS FOR CLINICAL PULSE WAVE VELOCITY ESTIMATION

Device	Cost-effectiveness	"One-step" method	Reliability
Athos	+	+	+
SphygmoCor	-	-	+
PulsePen	-	-	-
Complior	-	+	-

+ : advantageous w.r.t. the others
- : disadvantageous w.r.t. the others

This article is organized as follows. In section II the Athos system is described: the hardware, the software, and the clinical user procedure. Section III contains the validation results obtained comparing the proposed system with the clinical gold standard device for the PWV extraction. Finally, in Section IV some conclusions are drawn up.

II. PROPOSED SYSTEM

The Athos prototype for noninvasive PWV evaluation is mainly composed of a hardware unit that manages the signals acquisition and a specific laptop application that processes the acquired data and provides a graphical representation to the clinical operator. The entire system has been developed in order to be compliant with the clinical safety rules and guidelines described in the IEC-60601 standard for medical devices [18]. Furthermore, although the system performs the PWV one-step measurement, it offers the possibility to be interfaced with an external clinical-grade ECG device. This choice allows doctors to monitor the patient's health condition and, in addition, to have the opportunity to compare the resulted PWVs both with the direct differential PTT and with the two-steps method (provided by the gold standard instrument, still based on ECG).

A. The hardware

The Athos device consists of a main unit that manages and synchronizes all the signal acquisitions. With this system, there is the possibility to simultaneously acquire two pulse waves together with the ECG signal coming from the EDAN SE-1

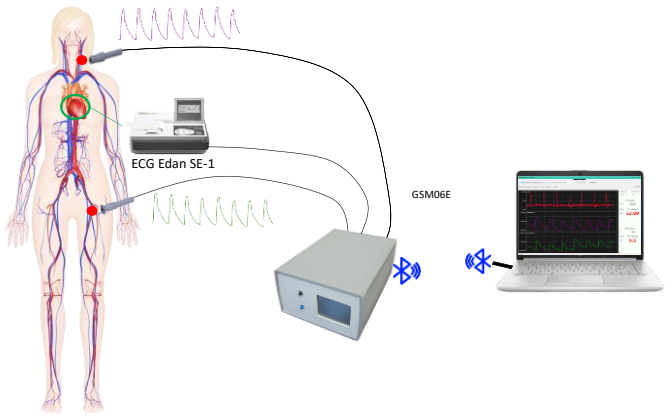

Fig. 1. Athos device summary scheme. It is composed by the main unit, that collects the two pulse waves and the electrocardiogram, and the software interface, running on the operator laptop. The device and the computer are connected through low energy v4.1 Bluetooth.

Fig. 2. Athos main device unit. On the left: the unit front panel, with the LCD (which shows the state of the sensors, their sample frequencies and the Bluetooth link state) and the button for the system reset. On the right: the internal interconnections between the STM32F429 Discovery Kit and the other system components.

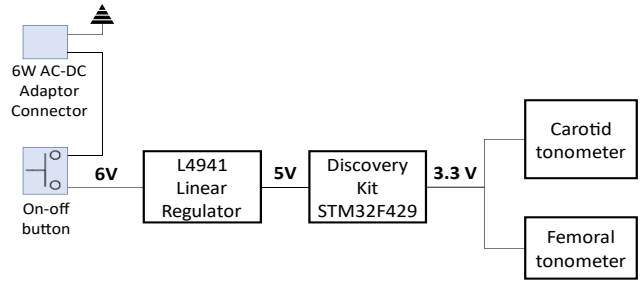

Fig. 3. Power supply scheme: from the 6W AC-DC Adaptor to the 3.3V voltage supply for the tonometers.

Fig. 4. On the left: pressure MEMS sensor for pulse wave acquisitions. On the right: 3d-printed pen supports for the MEMS sensor (on the top the femoral, on the bottom the carotid support).

electrocardiograph (Edan, Shenzhen, China) (Fig. 1).

To fulfill the compliance with the IEC-60601-1 standard, the acquisition unit is powered by a 6W AC-DC adaptor (GSM06E Mean Well). This power supply is specially designed for medical equipment because it implements double isolation with respect to the AC power supply. In addition, all the connectors for cables and panels were chosen to ensure a safe connection, avoid misconnections, and be suitable for medical applications.

The entire acquisition system is managed by an STM32F429 Discovery Kit (STMicroelectronics, Shanghai, China) and placed into the main unit (Fig. 2). This board hosts a STM32F429ZIT6 microcontroller, a 32-bit high-performance Micro-Controller Unit (MCU) part of the STM32F4 family and based on the ARM Cortex-M4 core. The adopted Discovery Kit also includes a 2.4" LCD that is used to give the operator useful information about the sensors and the status of Bluetooth Low Energy (BLE) wireless connection (Fig. 2). To power the discovery board, starting from the 6V voltage given by the external power supply, a linear voltage regulator provides the required 5V. When the discovery board is switched on, it generates a 3.3V voltage useful to power the MEMS sensors for the pulse wave signals detection (Fig. 3). The STM32F429 Discovery kit also offers two microswitches that could be programmed to give a direct command to the MCU. Both the buttons are made accessible on the device front panel and they could be pressed by the operator to reset the system. Moreover, there is a switch to turn on or off the entire device in the back panel.

The arterial pulse signal is acquired by a MEMS pressure sensor (Fig. 3), the LPS35HW (STMicroelectronics, Shanghai, China), that has been configured as a force sensor (tonometer) for this specific application. If placed on the skin in proximity of the arterial vessel, this sensor lets to detect the alteration of the superficial tension generated by the blood pulse inside the artery. As reported in the literature and described by the Laplace law, this variation is strongly linked to the change of the blood pressure occurring inside the vessel [19]. Through this sensing, it is possible to collect the pulse wave generated by the systolic ejection on different body locations.

The two MEMS sensors were placed into two 3D-printed supports to facilitate the sensor usage, made with a specific resin for clinical use (Fig. 4, right side). In order to obtain some probes that easily give stable and reliable signals, several supports of different types and forms were tested with the help of the medical staff. The dimensions, shape, and terminal part profiles were modified to get the carotid and femoral best pulse waves, respectively. The pen-shaped supports that simplified operator handling and provided the most desirable results were selected. The carotid probe terminal part is sharper to be kept as a pen, whereas the femoral one is flatter to be placed among the operator's left-hand fingers. In this way, a stable simultaneous sensors placement is possible, leading to better signals capture.

The two sensors used for the arterial pulse acquisition provide a digital output. They are interfaced to the MCU core using two SPI (Serial Peripheral Interface) ports, configured in a 3-wire communication protocol.

Concerning the ECG, the SE-1 Edan electrocardiograph device was chosen to be part of the system because it can output the acquired ECG signal through an external input/output connector. A simple interface circuitry has been developed to adjust the ECG output signal to be compliant to the characteristics of the MCU embedded Analog to Digital Converter (ADC) and take advantage of its input dynamic range.

With the purpose to ensure the galvanic isolation of the subject, the acquisition unit is controlled by the operator laptop through a wireless interconnection. On the PC, the developed software interface helps the operator to find the correct placement of the sensors, to monitor the quality level of the collected signals, and to save them for further analysis. The selected wireless module is the SPBTLE-RF (STMicroelectronics, Shanghai, China) that integrates BLE radio operating at 2.4 GHz (Bluetooth specification version 4.1). It provides a low power data transmission up to 10m, guaranteeing a safe distance between the laptop and that the main unit (full compliancy with the IEC-60601). This module is interfaced with an SPI port of the STM32F429 MCU and it

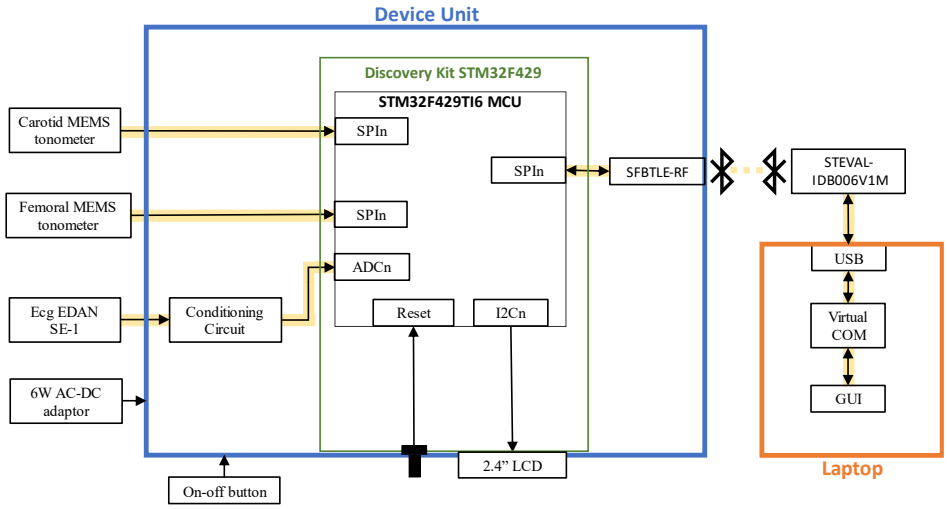

Fig. 5. Block diagram of Athos system. The MCU, included in the Discovery Kit, manages and synchronizes the acquisition of three different signals (two digital tonometers and one analog ECG from the Edan SE-1) and the Bluetooth transmission of the collected data (through the SFBTLE-RF). The data flow path is highlighted in yellow: from the sensors to the graphical user interface in the user laptop.

establishes a connection with a STEVAL-IDB006V1M module (STMicroelectronics, Shanghai, China), plugged into the operator PC through a USB port. For the real-time data transmission, an ad-hoc protocol was developed and implemented in order to take advantage of the full Bluetooth bandwidth.

The system interconnections are reported in Fig. 5, where it is possible to see how the signals move from the acquiring sensors to the laptop GUI through Bluetooth communication. To better synchronize both the digital output of MEMS pressure sensors and the analog ECG signal, the MCU sampling frequency is set at 680 Hz, which ensures a temporal resolution of 1.5 ms. Considering the tonometer maximum sampling frequency of 170 Hz, to synchronize the system signals acquisition, the MCU performs the sensors readings every four ADC conversions (170x4=680). Captured data are put on a buffer that contains *7* samples from each tonometer and *28* (7x4) ECG values, which is then sent through the wireless link.

B. The software algorithm

By means of the Bluetooth-LE wireless module and the firmware specifically created, data arrive from the acquisition system to the USB-port-dongle. A virtual serial communication (COM) port is then created on the laptop and, thanks to this, the GUI is able to receive and manage the data sent from the main acquisition unit.

When a new transmitted buffer is available, this is unpacked and the three signals (femoral pulse wave, carotid pulse wave, and ECG) are placed into three dedicated circular buffers. To synchronize the visualization of the signals the different sampling frequencies must be considered. For this reason, the tonometer waveforms are resampled at 680Hz to be coherent with the ECG sampling frequency. These three buffers are used to update the signals visualization in the GUI window (Fig. 6).

Besides the data visualization, the dedicated interface lets to store the data that later are processed to extract the PWV through a dedicated method in Matlab environment. The goal of the algorithm implemented in Athos is to extrapolate on each cardiac cycle the feature that lets to detect the blood pulse passage. For this purpose, the intersecting tangent method is addressed. It is essentially the signal "foot" extrapolation, that corresponds to the point delineated by the projection on the signal of the intersection between a horizontal line, passing through the minimum before the start of the systolic peak, and the tangent to the point of maximum first derivate (Fig. 7d). As demonstrated by Chiu et al. [20], this characteristic of the pulse resulted to be the most reliable among all the features that could be extracted in the arterial pulse (such as minimum, maximum, first derivate point, etc.).

The algorithm implementation for the intersecting tangent point detection includes several filters steps for removing the DC-bias, for evaluating the heartbeat frequency and, by consequence, the cardiac period of the subject under investigation. Several filter types were evaluated, but the ones that resulted to be more effective are the biquadratic filters, which correspond to a second order recursive linear filter (containing two poles and two zeroes). This choice was done because, unlike all the other digital filter architectures, their structure lets to obtain less signal distortion with a more efficient computational implementation. Furthermore,

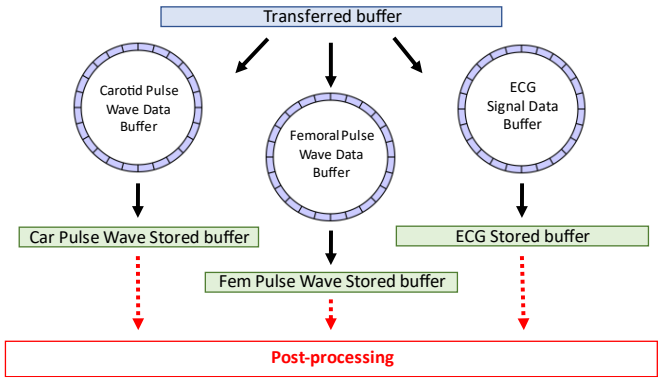

Fig. 6. GUI data flow. The transferred buffer, that arrives via Bluetooth, is processed and distributed in the three circular buffers (carotid pulse wave, femoral pulse wave and ECG signal), used for the signals plot in the window. The data are then stored in three buffers for the post-processing.

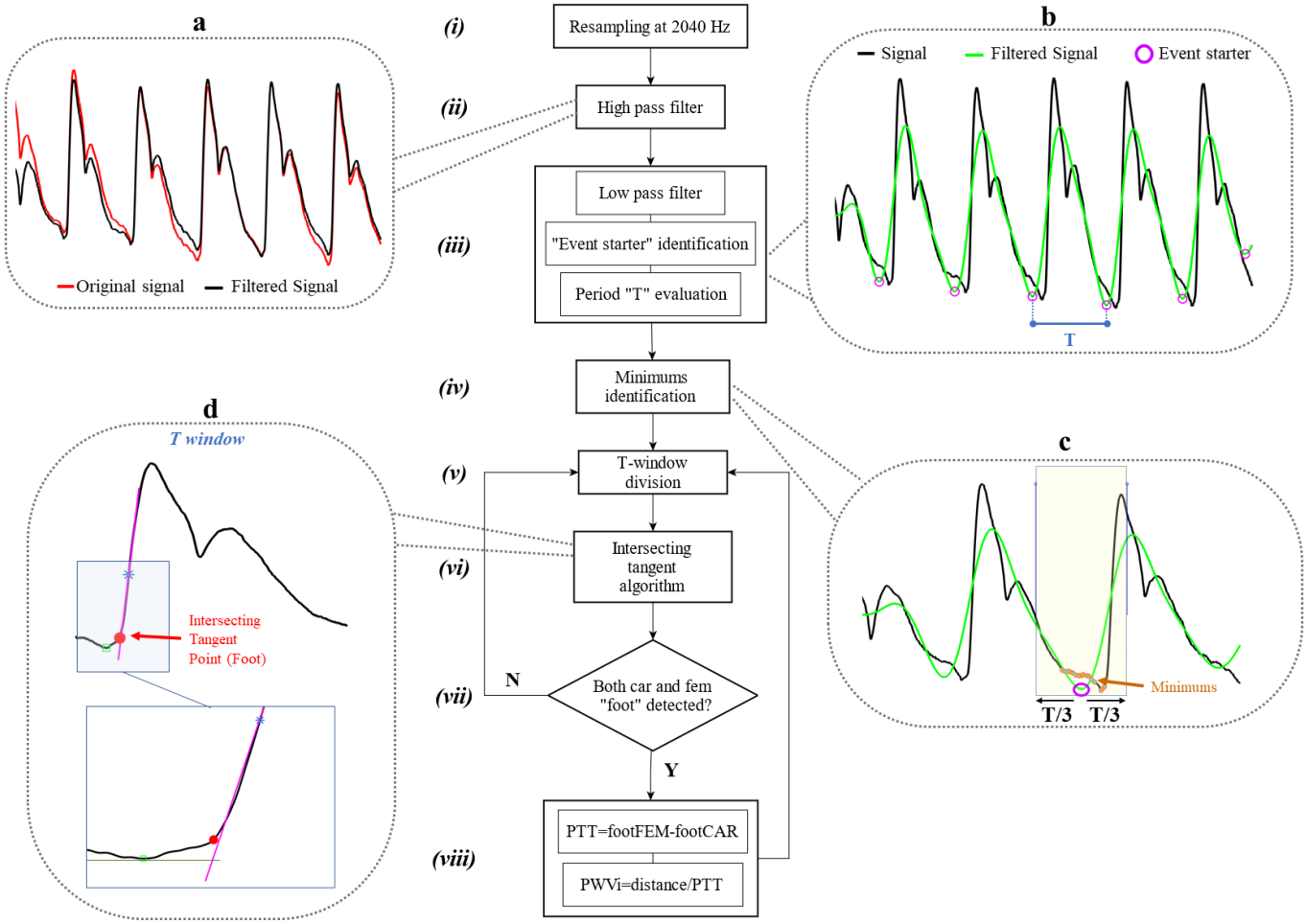

Fig. 7. Algorithm steps for the "intersecting tangent" feature extraction.

considering the frequencies involved in our system, they introduce a low phase delay and avoid numerical non-convergence issues.

Specifically, each filter-step is implemented by a zero-phase forward and reverse four stages biquadratic filter: the signal is reversed, it is filtered with a biquadratic filter for the first time and then, after a second reversion, it is again filtered. Each reversion means rearranging the order of the samples contained in the signal by putting the elements in the backward order. The double filtering approach avoids phase shift and ensures the temporal alignment between the pre- and the post- filtered signals. Specifically, the applied Biquadratic Cascade IIR Filters uses a direct form II transposed structure, in which every biquadratic stage implements a second-order filter using the following difference equation:

$$y[n] = b0 * x[n] + d1 \quad (2)$$

Where:

$$d1 = b1 * x[n] - a1 * y[n] + d2 \quad (3)$$

$$d2 = b2 * x[n] - a2 * y[n] \quad (4)$$

Here below, the steps addressed to extrapolate the cf-PTT of the collected signals and implemented in Matlab are described in detail, while Fig. 7 provided an overview of the entire procedure.

(i) In order to have a system with a high time resolution of the extracted PTT, the tonometer signal is resampled to 2040Hz through a cubic spline. As a result of this resampling, the signal time resolution is 0.5 ms, which is remarkably higher than before. The adopted interpolation is done through a third-degree polynomial with a forced continuity in the second derivate.

(ii) To remove the signal DC-offset, a high pass filter of 4th order with a cut-off frequency of 0.5 Hz is applied (Fig.7a).

(iii) A 4th order low pass filter at 2 Hz is then applied to identify the numbers of events (blood pulses) that occurred in the pulse wave under evaluation (Fig. 7b). All the relative minimums of the low pass filtered signal are considered as the *event starters*, i.e. the array index corresponding to the initial of each blood pulse. Afterward, the cardiac period *T* is defined as:

$$T = \frac{1}{n-1}\sum_{i=1}^{n-1}(event\ starter_{i+1} - event\ starter_i) \quad (5)$$

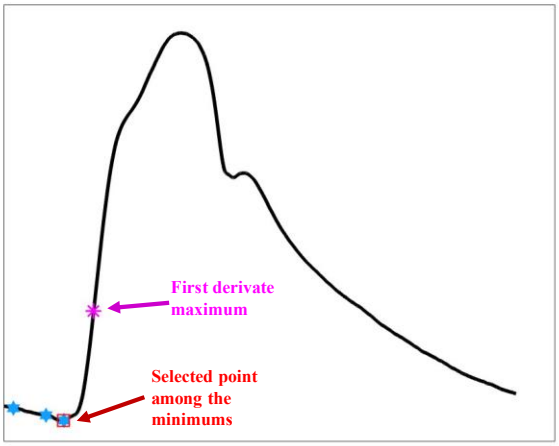

Fig. 8. Choice of the right minimum for the intersecting tangent algorithm among all the minimums detected before the rising edge of the pulse. The one closest to the point of first maximum derivate is chosen.

Where *n* is the number of the identified *events starters* and *T* represents the number of samples in the mean cardiac period.

(iv) Starting from each *event starter*, only a ±*T*/3 signal portion is considered, where *T* is the number of samples that are part of the cardiac period, evaluated in the previous step. In this interval, all the minimums are identified with the purpose of classifying the ones located at the foot of the pulses rising edges and finding the useful one for the intersecting tangent features extraction. A threshold is defined as 50% of the lowest minimum's y-coordinate among all the detected. So, if the $y_{\min\,(i)} < threshold$ the relative minimum is saved in the "minimums buffer". It has to be underlined how, due to the signal noise, before the starting of the rising edge usually more minimums are found out each pulse (Fig. 7c).

(v) To proceed with the "foot" extraction each blood pulse must be considered separately. For this, starting from every *event starter* a window of *T* samples has to be separately examined (*T-window*).

(vi) In the selected *T-window*, the intersecting tangent point extraction is performed. The first derivate of the signal is computed then, starting from each relative minimum extracted in the step (*iv)*, the first maximum of the first derivate is identified. All the minimums detected before the rising edge of the pulse merge in the same maximum derivate point that is so determined. Considering that for the feature extraction one point of minimum is needed, the nearest to the maximum slope of the edge is taken (Fig.8). At this point, both the tangent passing through the maximum of the first derivate and the horizontal line through the minimum are traced. Finally, the intersection between the two lines is projected on the signal and that is the "foot" of the pulse rising edge (Fig. 7d). The foot x-coordinate is saved in carotid o femoral "features vectors".

(vii) If both the processing of the carotid and the femoral pulse waves lead to the feature detection the PTT is evaluated:

$$PTT = foot_{fem} - foot_{car} \tag{6}$$

and then the PWV:

$$PWV = \frac{distance_{fem-car}}{PTT} \tag{7}$$

(viii) The process restarts from the first step *(v)* considering a new window of *T* samples.

C. The PWV acquisition procedure

The Athos operator interface was designed in Visual Studio environment, using *C#* as programming language and DirectX Application Programming Interface. It lets to visualize the acquired signals and to guide the operator in a good quality PWV assessment through some expedients that will be explained in this paragraph.

When the software interface is launched, a first "Study and Patient Data" window appears. In this form, the operator has to insert data regarding the subject under analysis: the identification code (to associate the patient with the trial), the values of systolic and diastolic blood pressures, and the *cf-distance*, i.e. the distance measured between the femoral and the carotid acquisition points. In order to assess the value of the blood pulse velocity, the Matlab algorithm considers this *cf-distance* value multiplied by 0.9 because it has been shown how this value is the most correct and suitable for PWV extraction [21], [22]. Usually, operators perform the distance measurement by using a common tape and projecting in the air the acquisition sites' positions to avoid body protuberances.

After this data insertion, it is possible to open the acquired signals in the "acquisition window" (Fig. 9), to start with the evaluation. The two pulse waves are displayed by default, whereas ECG visualization is optional. Signals are drawn on the screen and every five seconds they refresh. The visualization time of each screen can be changed by putting a different duration period in the specific box on the window.

To better address a good quality signal acquisition and so a more reliable PWV assessment, the Athos interface is provided with a peculiar pulse waves plot: the visualization starts with the zoom only when the signals have an amplitude higher than 400 mV_{pp}. This expedient lets to better achieve a high Signal Noise Ratio of the tonometer signals, which means more stability and less noise corruption in the parameter evaluation. On the other hand, if they have a too large amplitude, they are dynamically refitted on the screen. Moreover, to help the operator to understand the signal quality, two white lines are placed to guide the user to obtain a reasonable signal amplitude in each graph. It is recommended to have a signal that is as big as the amplitude defined by the two horizontal lines (Fig. 9).

Once the clinical operator has obtained good and stable signals for both the carotid and femoral waves for at least one minute, to finish the acquisition, the space bar has to be pushed. Whit this move, all the bio-signals and the study data (subject ID, distance values, etc.) are stored in a binary file that can be later read and processed through the algorithm, as explained in

the previous paragraph. To be more comparable as possible with the golden standard, for the PWV evaluation the Athos algorithm processes only the last ten seconds of the signals before the acquisition interruption. In addition, considering that the operator must remove the sensors from the subject and press the spacebar for the report generation, the system evaluates the ten-seconds-signals for the final processing discarding the last two seconds.

The "report window" is the final document of the subject's measurement, generated to better compare the results obtained with the Athos system and the ones with the Sphygmocor (Fig. 10). It displays the summary of the patient data, the single PTT values obtained in the last ten seconds, and the relative averaged PTT and PWV, with their standard deviations and percental standard deviation. Moreover, the system applies a further quality restriction by rejecting all the PTT values not included in the range sd±0.9*sd. After this, the final PWV is reassessed considering only the remaining PTTs. At the bottom of the report window, the signals are shown together with the extracted features. As in (1), the final PWV is obtained dividing the femoral-carotid distance, already multiplied for 0.9, for the mean cf-PTT in the last ten seconds.

III. SYSTEM VALIDATION

In order to validate the Athos system, a study was conducted in the Hospital of the "Città della Salute e della Scienza" in Turin (Italy). In this trial, approved by the "University of Turin Bioethical Committee", the performances given by Athos were compared with the one obtained with the SphygmoCor device, that is the clinical reference for noninvasive PWV assessment.

The study population was composed of 10 volunteer subjects, aged between 21 and 63 years, who accepted to be part of the trial. Table 2 details the physiological parameters of the people who took part in the study, that remained anonymous following the protocol. Two clinical operators carried out the acquisitions with the two instruments, interchanging the device between them for every subject (i.e. if for subject one the operator A used the Athos and the operator B used the SphygmoCor, for subject two the operator A was associated with the SphygmoCor and vice versa).

Following the study protocol, after the anamnesis information, the two operators identify the best carotid and

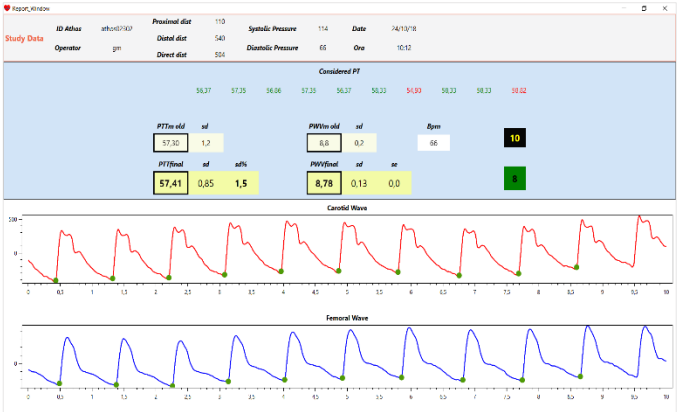

Fig. 10. "Report window" given as final summering output. On the top the patient data, in the middle the extracted parameters and on the bottom the collected signals with the extracted features are reported.

Fig. 9. "Acquisition window" with a refresh time of five seconds. It is noticeable how the pink signal (the carotid) is not big enough to be zoomed. Otherwise, the green (femoral), that is bigger than the white guidelines, does not saturate in the window.

femoral locations through tactile arterial palpation. Once located, the two spots are marked to be sure that the acquisition sites do not change for the two instruments. Then, through a measuring tape, the femoral-carotid distance is evaluated. As in the standard clinical procedure, this directly measured distance (in mm) is multiplied for a constant equal to 0.9. In fact, S. Huybrechts et al. in [23] explain how thanks to this correction the femoral-carotid distance better matches the real arterial pathway, which is surely different from the one resulting with the linear tape measurement approximation.

Afterward, the first operator starts with the SphygmoCor two-steps acquisition proceeding with the carotid pulse detection and subsequently with the femoral pulse. When the first PWV assessment is completed, the second operator goes ahead performing the femoral and carotid simultaneous acquisition with the Athos device. This procedure will be repeated three times on each subject, both for statistical purposes and also to be aligned with the common practice for clinical PWV evaluation; indeed, doctors usually consider the actual PWV value as the one obtained after the average of three consecutive acquisitions.

Once the acquisition is concluded and the data are processed, the generated report contains all the extracted parameters and the final cf-PWV, ready to be compared with the SphygmoCor estimation.

TABLE 2
PHYSIOLOGICAL PARAMETERS OF THE SUBJECTS

Subject	Age	Gender	Weight [kg]	Height [cm]	BMI [kg/m^2]
1	37	M	73	186	21.10
2	54	M	96	185	28.05
3	52	F	51	162	19.43
4	36	M	68	181	20.76
5	55	M	88	176	28.41
6	63	M	77	174	25.43
7	21	M	69	178	21.78
8	63	F	64	162	24.39
9	41	F	55	162	20.96
10	25	M	86	194	22.85

M: male, F: female

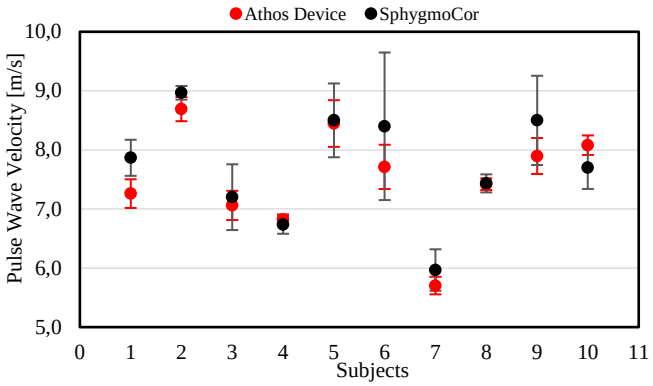

Fig. 11. PWVs final values obtained for the 10 subjects under analysis. These values are the result of an average on three tests for both the device, the error bars report the standard deviations.

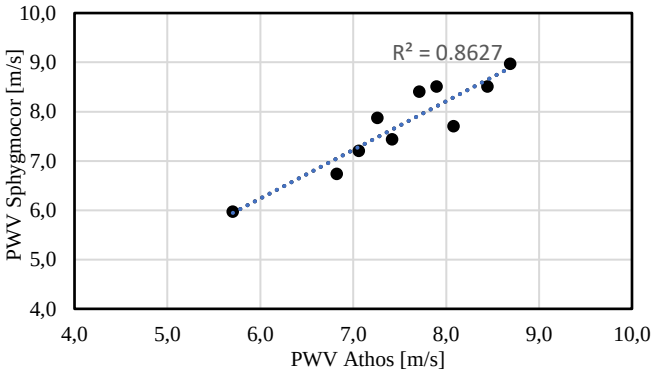

Fig. 12. Pulse wave velocity measurements with Athos (one-step method) versus SphygmoCor (two-steps method): the scatterplot shows a linear correlation between the values measured by the two instruments among all the subjects.

In Table 3 are summarized the PWVs collected by the two devices for all the analyzed subjects. The single tests are reported together with the averaged value and the relative standard deviation. From these, it is clear how the PWV measurements from the Athos device are highly comparable with the ones obtained through the gold reference. Furthermore, looking at the standard deviation, it is notable how the developed device has a higher repeatability.

In Fig. 11, the final PWVs values, averaged on three tests, are illustrated for the whole study population. The error bars represent the measurements dispersion and it is clear how the Athos system has a higher reproducibility in almost all the cases. In Fig. 12 is then depicted the resulted linear correlation computed on the final PWV values provided by both the devices.

The reported study was conducted in order to evaluate the quality, accuracy and reliability of the developed instruments; and according to the operators' feedback, the Athos system resulted easier to use with a very fast learning curve.

IV. CONCLUSIONS

To spread the adoption of PWV evaluation as a key parameter to assess cardiovascular risk, regardless of other well accepted risk factors, a significant cost reduction on adoptable measurement devices is strongly required. On the other hand, the quality, accuracy, and reliability of the provided results must be preserved together with a simple and fast examination approach based on a portable system.

In this work, a novel noninvasive system for clinical PWV estimation has been proposed. The presented solution covers all the aspects related to the parameter acquisition and many of them have been improved: starting from the sensing elements, going through the signal processing algorithms and up to the way the user interface bring the operator to a rapid and consistent result.

The system validation, performed on ten healthy volunteer subjects, showed a strong correlation with respect to the adopted gold standard reference equipment. It is also interesting to note that, in most cases, the acquired results related to the same subject demonstrate better quality and repeatability.

In conclusion, it was possible to prove how Athos is a truly cost-effective system that addresses fully reliable and easy to perform PWV estimations, potentially able to expand the availability of this measure and the fields of application.

TABLE 3
VALIDATION RESULTS

Subject	Test	PWV Athos Device [m/s]	Standard Deviation	PWV SphygmoCor [m/s]	Standard Deviation
1	1	7.5	0.1	7.6	0.4
	2	7.1	0.0	8.2	0.3
	3	7.1	0.1	7.8	0.4
	Mean	**7.3**	**0.2**	**7.9**	**0.3**
2	1	8.5	0.1	8.9	0.6
	2	8.6	0.2	8.9	0.7
	3	8.9	0.1	9.1	0.7
	Mean	**8.7**	**0.2**	**9.0**	**0.1**
3	1	7.0	0.2	7.1	0.4
	2	7.3	0.2	7.8	0.4
	3	6.9	0.1	6.7	0.3
	Mean	**7.1**	**0.25**	**7.2**	**0.6**
4	1	6.7	0.0	6.9	0.4
	2	6.8	0.1	6.6	0.4
	3	6.9	0.1	6.7	0.3
	Mean	**6.8**	**0.1**	**6.7**	**0.2**
5	1	8.8	0.1	9.2	0.3
	2	8.5	0.2	8.0	0.3
	3	8.0	0.1	8.3	0.4
	Mean	**8.4**	**0.4**	**8.5**	**0.6**
6	1	8.1	0.2	9.8	0.5
	2	7.3	0.1	8.0	0.7
	3	7.8	0.1	7.4	0.3
	Mean	**7.7**	**0.4**	**8.4**	**1.2**
7	1	5.5	0.1	5.6	0.2
	2	5.7	0.1	6.0	0.4
	3	5.8	0.1	6.3	0.3
	Mean	**5.7**	**0.2**	**6.0**	**0.4**
8	1	7.3	0.1	7.3	0.2
	2	7.5	0.1	7.4	0.3
	3	7.5	0.1	7.6	0.5
	Mean	**7.4**	**0.1**	**7.4**	**0.2**
9	1	8.1	0.1	9.2	0.6
	2	7.6	0.1	8.6	0.6
	3	8.0	0.1	7.7	0.4
	Mean	**7.9**	**0.3**	**8.5**	**0.8**
10	1	8.2	0.2	8.0	0.7
	2	7.9	0.1	7.8	0.6
	3	8.1	0.1	7.3	0.7
	Mean	**8.1**	**0.2**	**7.7**	**0.4**

REFERENCES

[1] G. Mancia *et al.*, "2013 ESH/ESC Guidelines for the management of arterial hypertension," *Eur. Heart J.*, vol. 34, no. 28, pp. 2159–2219, Jul. 2013, DOI: 10.1093/eurheartj/eht151.

[2] C. Vlachopoulos, M. O'Rourke, W. W. Nichols, M. O'Rourke, and W. W. Nichols, *McDonald's Blood Flow in Arteries: Theoretical, Experimental and Clinical Principles*. CRC Press, 2011.

[3] M. F. O'Rourke and G. Mancia, "Arterial stiffness," *J. Hypertens.*, vol. 17, no. 1, pp. 1–4, Jan. 1999.

[4] Safar Michel E., Levy Bernard I., and Struijker-Boudier Harry, "Current Perspectives on Arterial Stiffness and Pulse Pressure in Hypertension and Cardiovascular Diseases," *Circulation*, vol. 107, no. 22, pp. 2864–2869, Jun. 2003, DOI: 10.1161/01.CIR.0000069826.36125.B4.

[5] Kelly R, Hayward C, Avolio A, and O'Rourke M, "Noninvasive determination of age-related changes in the human arterial pulse.," *Circulation*, vol. 80, no. 6, pp. 1652–1659, Dec. 1989, DOI: 10.1161/01.CIR.80.6.1652.

[6] Cohn Jay N. *et al.*, "Noninvasive Pulse Wave Analysis for the Early Detection of Vascular Disease," *Hypertension*, vol. 26, no. 3, pp. 503–508, Sep. 1995, DOI: 10.1161/01.HYP.26.3.503.

[7] Resnick Lawrence M., Militianu Daniela, Cunnings Amy J., Pipe James G., Evelhoch Jeffrey L., and Soulen Renate L., "Direct Magnetic Resonance Determination of Aortic Distensibility in Essential Hypertension," *Hypertension*, vol. 30, no. 3, pp. 654–659, Sep. 1997, DOI: 10.1161/01.HYP.30.3.654.

[8] Lang R M, Cholley B P, Korcarz C, Marcus R H, and Shroff S G, "Measurement of regional elastic properties of the human aorta. A new application of transesophageal echocardiography with automated border detection and calibrated subclavian pulse tracings.," *Circulation*, vol. 90, no. 4, pp. 1875–1882, Oct. 1994, DOI: 10.1161/01.CIR.90.4.1875.

[9] J. Solà, O. Chételat, C. Sartori, Y. Allemann, and S. F. Rimoldi, "Chest pulse-wave velocity: a novel approach to assess arterial stiffness," *IEEE Trans. Biomed. Eng.*, vol. 58, no. 1, pp. 215–223, Jan. 2011, DOI: 10.1109/TBME.2010.2071385.

[10] B. Williams *et al.*, "2018 ESC/ESH Guidelines for the management of arterial hypertension," *Eur. Heart J.*, vol. 39, no. 33, pp. 3021–3104, Sep. 2018, DOI: 10.1093/eurheartj/ehy339.

[11] L. M. Van Bortel *et al.*, "Expert consensus document on the measurement of aortic stiffness in daily practice using carotid-femoral pulse wave velocity," *J. Hypertens.*, vol. 30, no. 3, pp. 445–448, Mar. 2012, DOI: 10.1097/HJH.0b013e32834fa8b0.

[12] T. Pereira, C. Correia, and J. Cardoso, "Novel Methods for Pulse Wave Velocity Measurement," *J. Med. Biol. Eng.*, vol. 35, no. 5, pp. 555–565, 2015, DOI: 10.1007/s40846-015-0086-8.

[13] S. Conoci, F. Rundo, G. Fallica, D. Lena, I. Buraioli, and D. Demarchi, "Live Demonstration of Portable Systems based on Silicon Sensors for the monitoring of Physiological Parameters of Driver Drowsiness and Pulse Wave Velocity," in *2018 IEEE Biomedical Circuits and Systems Conference (BioCAS)*, Oct. 2018, pp. 1–3, DOI: 10.1109/BIOCAS.2018.8584709.

[14] V. Bikia *et al.*, "Noninvasive Cardiac Output and Central Systolic Pressure From Cuff-Pressure and Pulse Wave Velocity," *IEEE J. Biomed. Health Inform.*, vol. 24, no. 7, pp. 1968–1981, Jul. 2020, DOI: 10.1109/JBHI.2019.2956604.

[15] M. Butlin and A. Qasem, "Large Artery Stiffness Assessment Using SphygmoCor Technology," *Pulse*, vol. 4, no. 4, pp. 180–192, Jan. 2017, DOI: 10.1159/000452448.

[16] P. Salvi, G. Lio, C. Labat, E. Ricci, B. Pannier, and A. Benetos, "Validation of a new noninvasive portable tonometer for determining arterial pressure wave and pulse wave velocity: the PulsePen device," *J. Hypertens.*, vol. 22, no. 12, pp. 2285–2293, Dec. 2004.

[17] F. Stea, E. Bozec, S. Millasseau, H. Khettab, P. Boutouyrie, and S. Laurent, "Comparison of the Complior Analyse device with Sphygmocor and Complior SP for pulse wave velocity and central pressure assessment," *J. Hypertens.*, vol. 32, no. 4, pp. 873–880, Apr. 2014, DOI: 10.1097/HJH.0000000000000091.

[18] "IEC 60601-1 - Medical electrical equipment - Part 1: General requirements for basic safety and essential performance." https://webstore.iec.ch/publication/2603.

[19] N. Ranganathan, V. Sivaciyan, and F. B. Saksena, *The Art and Science of Cardiac Physical Examination: With Heart Sounds and Pulse Wave Forms on CD*. Humana Press, 2007.

[20] Y. C. Chiu, P. W. Arand, S. G. Shroff, T. Feldman, and J. D. Carroll, "Determination of pulse wave velocities with computerized algorithms," *Am. Heart J.*, vol. 121, no. 5, pp. 1460–1470, May 1991, DOI: 10.1016/0002-8703(91)90153-9.

[21] A. L. Wentland, T. M. Grist, and O. Wieben, "Review of MRI-based measurements of pulse wave velocity: a biomarker of arterial stiffness," *Cardiovasc. Diagn. Ther.*, vol. 4, no. 2, pp. 193–206, Apr. 2014, DOI: 10.3978/j.issn.2223-3652.2014.03.04.

[22] T. Weber *et al.*, "Noninvasive determination of carotid–femoral pulse wave velocity depends critically on assessment of travel distance: a comparison with invasive measurement," *J. Hypertens.*, vol. 27, no. 8, pp. 1624–1630, Aug. 2009, DOI: 10.1097/HJH.0b013e32832cb04e.

[23] S. A. M. Huybrechts *et al.*, "Carotid to femoral pulse wave velocity: a comparison of real travelled aortic path lengths determined by MRI and superficial measurements," *J. Hypertens.*, vol. 29, no. 8, pp. 1577–1582, Aug. 2011, DOI: 10.1097/HJH.0b013e3283487841.